Christina Hagen*, Pragathi Gurumurthy and Thorsten M. Buzug

Effects of replacing the nasal cavity with a simple pipe like structure in CFD simulations of the airflow within the upper airways of OSA patients with patient individual flow rates

Abstract: OSA is characterized by repetitive collapses of the upper airways during sleep. Computational fluid dynamics can be used to investigate the abnormal pressure distribution in the patient's airways. The computational costs and model reconstruction effort can be reduced by focusing the simulations on the pharynx and replacing the nasal cavity by a simple pipe structure. In this work, the effects of the mentioned replacement on the simulated flow are evaluated. Airflow simulations using the k-ω turbulence model are performed in the anatomically correct airway of a patient having a high difference in the inspiratory volume flow rates of both nostrils, as well as in a model with replaced nasal cavity by a simple pipe structure. The simulated pressure distributions of both models are in very good agreement indicating the acceptability of replacing the nasal cavity by simple pipe structures in in-silico airflow analyses of OSA patients.

Keywords: Computational fluid dynamics, obstructive sleep apnea syndrome, OSA, upper airways, airflow.

https://doi.org/10.1515/cdbme-2017-0168

1 Introduction

The obstructive sleep apnea syndrome (OSA) is a common sleep-related breathing disorder that affects up to 23.4 % of women and 49.7 % of men [1]. It is characterized by repetitive closure of the pharyngeal lumen due to reversible soft tissue deformation resulting in cessations in breathing. The patients suffer from a disturbed sleep, daytime sleepiness and have a higher risk for cardiovascular diseases and depression.

Pharyngeal collapses are caused by a combination of the loss of tone in the upper airway musculature during sleep and the aerodynamic forces promoting the collapse [2]. A narrow airway is an anatomical feature predisposing for OSA [3-4]. The pathophysiological airflow situation due to anatomical predisposition of the airway can be investigated using airflow simulations in the upper airways by performing computational fluid dynamics (CFD). CFD analyses can become a powerful tool in diagnosis and therapy planning of OSA. For example, it has been shown with CFD that invasive mandibular distraction leads to a reduction in the upper airway resistance [5], and wearing of mandibular advancement appliances reduces the pressure drop in the human pharynx [6].

The area of interest for investigations of OSA phenomena is the pharynx as it is the collapsing part. The nasal cavity is often assumed to contribute to the upper airway flow as inspiratory airflow conditioner giving rise to turbulences that are conducted to the following airway path. The nasal cavity has a very complex shape that is difficult to reconstruct from tomographic images and it has a very complex flow pattern [7]. Hence, it is hard to acquire fully accurate numerical simulations of the nasal airflow and it dramatically increases the computational costs of the simulation. Due to these limitations the nasal cavity is often excluded in numerical simulations of upper airway flow [5-6]. It is important to validate the effects of omitting the nasal cavity on the flow features in the pharynx, especially on the acting pressure forces. In [8] it has been shown, that omitting the nasal cavity decreases the precision of flow modelling in the pharyngeal part, but replacing the nasal cavity by a simple pipe results in neglectable changes of the flow patterns in the pharynx. But, the numerical simulations in [8] were performed with steady flow conditions and a non-patient-specific inflow rate of 21.2 L min^{-1} equally

***Corresponding author: Christina Hagen:** University of Lübeck, Institute of medical engineering, Ratzeburger Allee 160, 23562 Lübeck, Germany, e-mail: hagen@imt.uni-luebeck.de
Pragathi Gurumurthy, Thorsten M. Buzug: University of Lübeck, Institute of medical engineering, Ratzeburger Allee 160, 23562 Lübeck, Germany, e-mail: gurumurthy@imt.uni-luebeck.de, buzug@imt.uni-luebeck.de

Open Access. © 2017 Christina Hagen et al., published by De Gruyter. This work is licensed under the Creative Commons Attribution-NonCommercial-NoDerivatives 4.0 License.

Unauthenticated
Download Date | 8/22/19 9:53 PM

distributed through both nostrils, although nasal obstructions have been identified as predisposing factor for OSA [9]. The investigation misses the patient-specific contributions of individual flow rates especially for significant differences in left to right nostril ventilation typical for nasal obstructions.

In the present study, the investigation of simplifying the nasal cavity by pipes from [8] is extended to one subject with patient specific inspiratory flow rates that are significantly different from the left to the right side. This is performed by analysing the results of steady numerical simulations in the patient-specific upper airway geometry including the nasal cavity with patient individual different left and right nostril inspiratory flow rates in comparison to the anatomically accurate pharyngeal and laryngeal parts extended by a simple pipe structure replacing the nasal cavity and using the sum of each nostril flow rate as inlet boundary condition.

2 Material and methods

2.1 Subject

The subject considered in this study was a 39 year old man with BMI of 26.2 and moderate sleep apnea (23 apnoic events per hour). The subject was recruited from patients undergoing surgery for placing a hypoglossal nerve stimulation device. This patient was chosen due to his ride side nasal obstruction. By rhinomanometry a mean inspiratory flow rate of 141 mls^{-1} for the right side and of 263 mls^{-1} for the left side were determined pre-operatively accompanied by a pressure loss of 35.1 Pa over the nasal cavity. A drug deswelling the nasal mucosa has been given to the patient before the measurement to ensure that no temporarily swelling of the mucosa affects the measurement.

2.2 Airway model reconstruction

An MR image of the subject was acquired using a 1.5 T MR unit (Achieva, Philips Medical Systems, Amsterdam, The Netherlands). 228 transversal slices with a slice spacing of 1.3 mm were generated, each slice consisting of 320×320 pixels with a pixel spacing of 0.78 mm × 0.78 mm. The open source software ITK-SNAP [10] was used for a manual segmentation of the airway and the generation of a surface representation, see figure 1. A second model was generated using the surface representation of the first model by cutting the airway in the nasopharyngeal part and replacing the nasal cavity by a simplified extension of 80 mm length forming a circle of 15 mm diameter at the inlet.

2.3 Airflow simulation

The flow within the human upper airways is in the laminar-to-turbulent transitional regime. Therefore, turbulence modelling is adopted for the airflow simulation. The Reynolds averaged Navier-Stokes (RANS) equations

$$\rho(\boldsymbol{u}\cdot\boldsymbol{\nabla})\boldsymbol{u} = \boldsymbol{\nabla}\cdot[-p\boldsymbol{I} + (\mu+\mu_T)(\boldsymbol{\nabla u} + (\boldsymbol{\nabla u})^T)] \quad (1)$$

$$\rho\boldsymbol{\nabla}\cdot\boldsymbol{u} = 0 \quad (2)$$

are used, where $\boldsymbol{u}$ is the velocity vector, p pressure, $\boldsymbol{I}$ identity matrix, μ dynamic viscosity of air ($\mu = 1.814\cdot10^{-5}$ Pa·s) and ρ its density ($\rho = 1.204$ kgm^{-3}). These are averaged versions of the conservation laws of mass and momentum suited for Newtonian fluids. The turbulence effects are incorporated by the eddy viscosity, μ_T. The eddy viscosity is modelled by the two-equation turbulence model k-ω, so that

$$\mu_T = \rho k\omega^{-1}, \quad (3)$$

where k is the turbulent kinetic energy and ω the specific dissipation rate.

In both models three different boundary conditions are applied:

- Zero pressure outlet boundary conditions,
- no-slip conditions at the airway walls and
- velocity inlet conditions $\boldsymbol{u} = \dot{V}A^{-1}$ with 5 % turbulence intensity, where $\dot{V}$ is the inlet volume flow rate and A the inlet area. In this case the flow rate is
  - $\dot{V} = 263$ mls^{-1} for the left nose inlet and $\dot{V} = 141$ mls^{-1} for the right nose in the case of the model with nasal cavity and
  - $\dot{V} = 404$ mls^{-1} for the circular inlet of the simplified model.

The governing equations are discretized with the finite element method. The discretized equations are numerically solved using a segregated solution process solving for the velocity and the pressure on the one hand and the turbulence variables k and ω on the other hand separately by a damped newton algorithm. The grid independence has been approved by demanding a change in the maximal flow velocity of smaller than 1 %. Equation (1) is only dependent on the gradient of the pressure, so a shift of the pressure has no influence on the other flow parameters. Hence, the equations can be solved using the zero pressure outlet boundary condition and the pressure is shifted afterwards so that the pressure at the beginning of the nasopharynx matches the patient specific pressure of -35.1 Pa. The simulations were computed using the commercial available software COMSOL Multiphysics (COMSOL Inc.).

Unauthenticated
Download Date | 8/22/19 9:53 PM

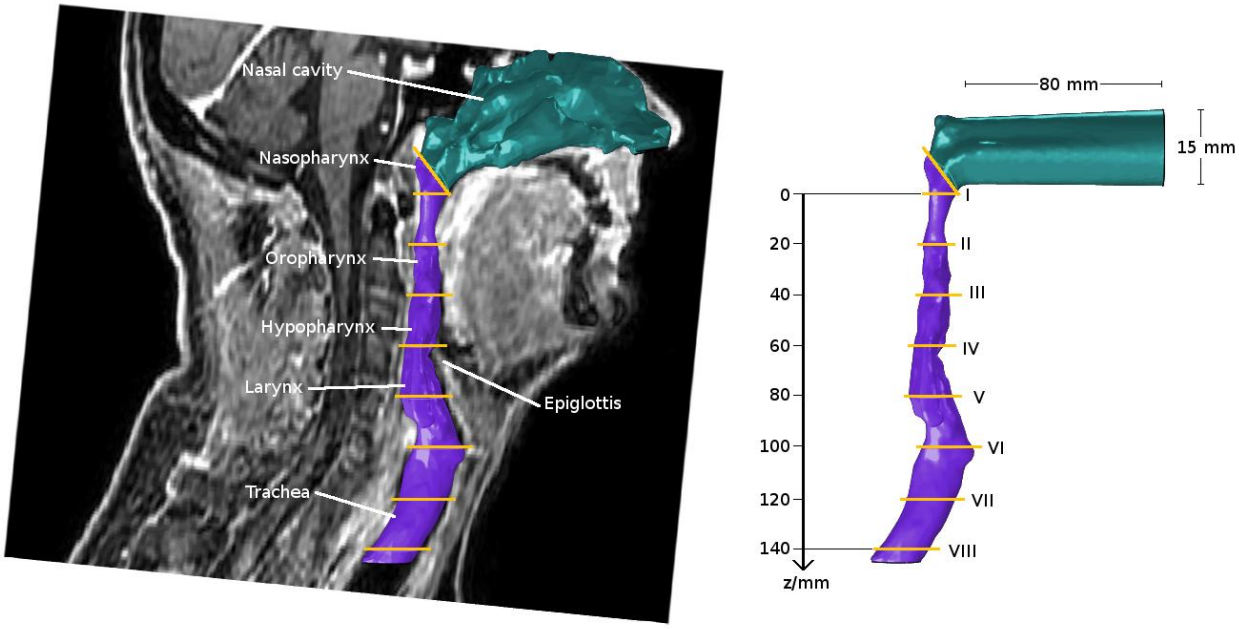

Figure 1: On the left hand side, a sagittal slice of the MR image is shown and the anatomically accurate model of the nasal cavity. On the right hand side, the model with simplified inlet area is depicted.

3 Results

The pressure distribution resulting from the airflow with patient-specific inspiratory flow rates is simulated. For the evaluation, eight different planes (I-VIII) along the pharynx and larynx are chosen. The positions of these planes are depicted in figure 1.

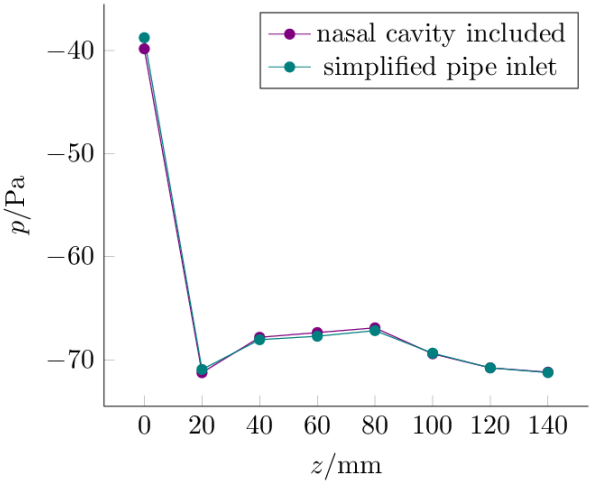

Figure 2: The mean pressure of eight planes along the pharynx is shown for both models.

The mean pressure values for these planes are plotted in figure 2 against the distance to the first plane. An image of the surface pressure distribution of both models is given in figure 3.

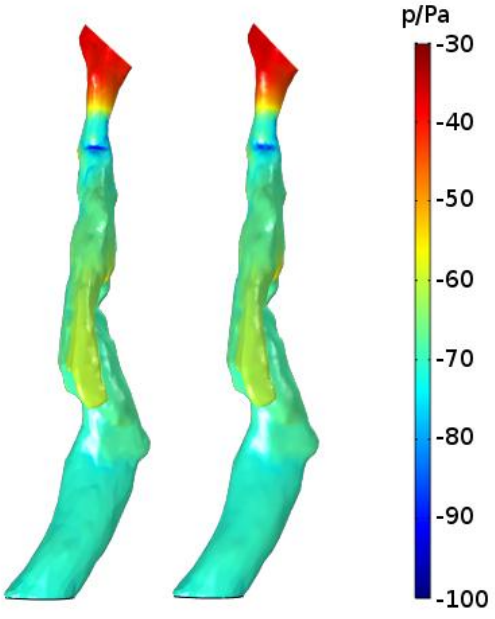

Figure 3: The surface pressure distribution in the pharyngeal and laryngeal part is depicted for the model including the

Unauthenticated
Download Date | 8/22/19 9:53 PM

nasal cavity on the left hand side and with simplified pipe inlet on the right hand side.

4 Discussion

The surface pressure depicted in figure 3 shows a great pressure drop in a small region from the end nasopharyngeal to beginning oropharyngeal part in both models. This pressure drop is also indicated by the mean pressures in the different planes. The pressure drops approximately about 30 Pa from plane I to plane II. The surface pressure also shows a small area of very high negative pressure of about -100 Pa that could correspond to the area of collapse.

There are no significant differences in the simulated pressure distributions of both models. The maximal difference of the mean pressure values along planes I to VIII is 2.7 % in plane I, which is the nearest one to the inlet area. The mean differences along the planes is 0.6 %.

The meaningful pressure drop in its spatial distribution as well as in its quantity is in very good agreement in both modelled geometries.

5 Conclusion

The replacement of the nasal cavity by a simple pipe structure does not significantly affect the pressure distribution in airflow simulations of patients with nasal obstructions having high differences in left to right nasal inspiratory flow rates.

The proposed replacement can therefore act as a powerful tool to decrease computational costs and effort of accurately reconstructing nasal cavity models and solving for the airflow within.

Acknowledgment: The authors like to thank the ENT department of the University Medical Centre Schleswig-Holstein (UKSH), especially Dr. Armin Steffen, for providing medical data.

Author's Statement

Research funding: This work is supported by the Graduate School for Computing in Medicine and Life Science funded by Germany's Excellence Initiative (DFG GSC 235/1). Conflict of interest: Authors state no conflict of interest. Informed consent: Informed consent has been obtained from all individuals included in this study. Ethical approval: The research related to human use complies with all the relevant national regulations, institutional policies and was performed in accordance with the tenets of the Helsinki Declaration, and has been approved by the authors' institutional review board or equivalent committee.

References

[1] Heinzer R, Vat S, Marques-Vidal P, Marti-Soler H, Andires D, Tobback N Mooser V, Preisig M, Malhotra A, Waeber G, Vollenweider P, Tafti M, Haba-Rubio J. Prevalence of sleep-disordered breathing in the general population: the HypnoLaus study. Lancet Respir Med 2015; 3(4):310-318.

[2] Isono S, Remmers JE, Tanaka A, Sho Y, Sato J, Nishino T. Anatomy of pharynx in patients with obstructive sleep apnea and in normal subjects. J Appl Physiol 1997; 82:1319-1326.

[3] Kim HY, Bok KH, Dhong HJ, Chung SK. The correlation between pharyngeal narrowing and the severity of sleep-disordered breathing. Otolaryng Head Neck 2008; 138:289-293.

[4] Schwab RJ, Pasirstein M, Pierson R, Mackley A, Hachadoorian R, Arens R, Maislin G, Pack AI. Identification of upper airway anatomic risk factors for obstructive sleep apnea with volumetric magnetic resonance imaging. Am J Resp Crit Care 2003; 168:522-530.

[5] Fan Y, Cheung LK, Chong MM, Chua HD, Chow KW, Liu CH. Computational fluid dynamics analysis on the upper airways of obstructive sleep apnea using patient-specific models. IAENG International Journal of Computer Science 2011; 38(4):401-408.

[6] Kluck C, Buzug TM. Numerical simulations of airflow in the human pharynx of OSAHS patients. Curr Dir Biomed Eng 2016; 1:552-555.

[7] Ito Y, Cheng GC, Shih AM, Koomullil RP, Soni BK, Sittitavornwong S, Waite PD. Patient-specific geometry modeling and mesh generation for simulating obstructive sleep apnea syndrome cases by maxillomandibular advancement. Math Comput Simulat 2010; 81:1876-1891.

[8] Cisonni J, Lucey AD, King AJC, Mohammed Shamsul Islam S, Lewis R, Goonewardene MS. Numerical simulation of pharyngeal airflow applied to obstructive sleep apnea: effect of the nasal cavity in anatomically accurate airway models. Med Biol Eng Comput 2015; 53:1129-1139.

[9] Lofaso F, Coste A, d'Ortho MP, Zerah-Lancner F, Delclaux C, Goldenberg F, Harf A. Nasal obstructions as a risk factor for sleep apnoea syndrome. Eur Respir J 2000; 16:639-643.

[10] Yushkevich PA, Piven J, Hazlett HC, Smith RG, Ho S, Gee JS, Gerig G. User-guided 3D active contour segmentation of anatomical structures: significantly improved efficiency and reliability. Neuroimage 2006; 31(3):1116-1128, www.itksnap.org.

Unauthenticated
Download Date | 8/22/19 9:53 PM